ISSN 1819-7140, Russian Journal of Pacific Geology, 2020, Vol. 14, No. 1, pp. 20–31. © Pleiades Publishing, Ltd., 2020.
Russian Text © The Author(s), 2020, published in Tikhookeanskaya Geologiya, 2020, Vol. 39, No. 1, pp. 24–36.

Age and Sources of Dzhagdy Terrane Metasedimentary Rocks in the Mongol–Okhotsk Fold Belt: Detrital Zircon U–Pb and Lu–Hf Isotopic Data

V. A. Zaika[a], * and A. A. Sorokin[a]

[a] *Institute of Geology and Nature Management, Far Eastern Branch, Russian Academy of Sciences, Blagoveshchensk, 675000 Russia*

**e-mail: zaika_v_a_88@mail.ru*

Received January 22, 2019; revised August 29, 2019; accepted September 6, 2019

Abstract—Ditrital zircon U-Pb and Lu-Hf isotopic data are reported for metaterrigenous deposits of Dzhagdy Terrane in the Mongol–Okhotsk Fold Belt. The youngest zircon populations in metasedimentary rocks of the Dzheskogon and Nekter formations is concluded to be of the Middle–Late Triassic and Early Jurassic Age, suggesting that the formations are Early Mesozoic and not Carboniferous, as was previously assumed. We have made the assumption that the Dzheskogon, Nekter, and Bochagor formations of the Dzhagdy Terrane are not a single sedimentary sequence, but a set of tectonic slices consisting of Late Paleozoic and Early Mesozoic rocks of differing genesis. This raises the question on whether the terrane under consideration is a fragment of an accretionary prism. Detrital zircon U-Pb geochronological and Lu-Hf isotopic data coupled with whole-rock Sm-Nd isotopic data from previous studies indicate that the sedimentary basin was mainly sourced from the continental Amur Superterrane (from the south in present-day coordinates). Material replenishment from the southern framing of the North Asian Craton (from the north in present-day coordinates) was either minimal or absent.

Keywords: metasedimentary rocks, U-Pb, Lu-Hf, Dzhagdy Terrane, Mongol–Okhotsk Fold Belt

DOI: 10.1134/S181971402001008X

The Mongol–Okhotsk Fold Belt is a significant structural element of East Asia. The belt is up to 300 km wide and extends 3000 km from the Uda Bay of the Okhotsk Sea to Central Mongolia (Fig. 1). Structurally, the belt, as of today, is a complex collage of tectonic blocks arranged along its strike, which are considered tectonostratigraphic areas [9, 15, 27] or terranes [9, 24, 49, 50].

The available paleomagnetic data in [11, 22, 45] evidence the appreciable distance between the southern margin of the North Asian Craton and the southern periphery of the Mongol–Okhotsk Belt continental mass as Paleozoic. These data, as well as the occurrence of Paleozoic and Early Mesozoic igneous associations within the belt and its flanking continental structures [1–3, 16, 20, 21, 25, 30–32, 36, 41, 54, 55, 57] evidence a long and complicated evolution of the belt.

Although many a generation of geologists have been studying the Mongol–Okhotsk Belt, many problems related to its evolution remain unresolved [24, 45, 49]. This arises primarily from the lack of geochronological and isotope–geochemical data, allowing boundary conditions for their development to be determined. In recent years, there has been progress in addressing these issues, which is related to obtaining primary data on the age of detrital zircons and Sm–Nd isotope–geochemical features of Mongol–Okhotsk Belt metasedimentary rocks. In particular, the belt was likely have subduction zones of different age and direction of subduction during the Paleozoic [33, 40, 44]. At the same time, the data are still insufficient in developing an integrated geodynamic model for the formation of the Mongol–Okhotsk Belt.

Thus, U–Pb and Lu–Hf isotopic studies have been carried out on detrital zircons from Paleozoic and Mesozoic metasedimentary rocks of the Dzhagdy Terrane (Fig. 1) in the Mongol–Okhotsk Fold Belt to determine age, as well as sources and source areas of terrigenous materials.

ANALYTICAL METHODS

Zircons were isolated using heavy liquids in the mineralogical laboratory of the Institute of Geology and Nature Management, Far East Branch of the Russian Academy of Sciences, Blagoveshchensk, Russia. Further, zircons were mounted in epoxy mounts, along with zircon standards (FC, SL, and R33), and polished halfway through individual zircon grains.

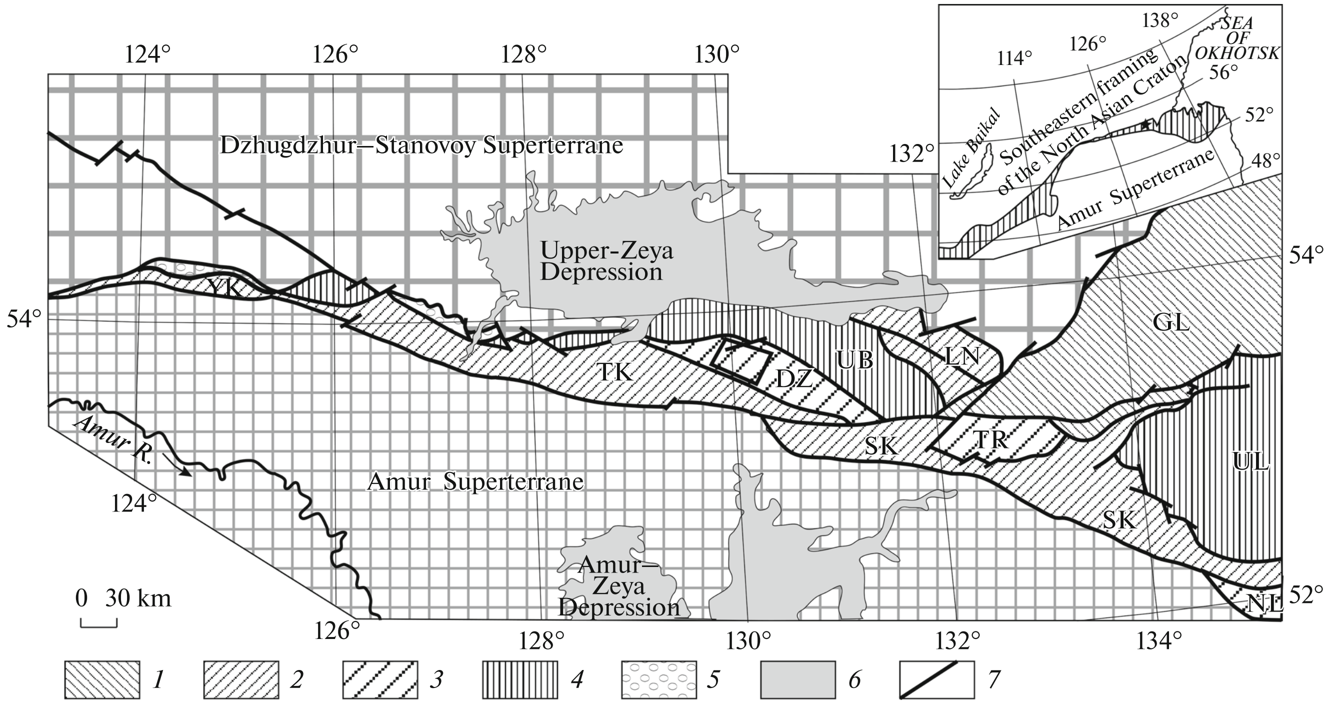

Fig. 1. Simplified structural zonation map of the eastern part of the Mongol–Okhotsk Fold Belt after [29]. *1*— terranes presumably composing Lower and Middle Paleozoic metasedimentary and metavolcanic assemblages; *2* — terranes presumably composing Middle and Upper Paleozoic metasedimentary and metavolcanic assemblages; *3*— terranes composing presumably Upper Paleozoic metasedimentary and metavolcanic assemblages; *4*—terranes composing presumably Lower Mesozoic turbidite assemblages; *5*—Upper Jurassic–Lower Cretaceous conglomerates, gravelstones, and sandstones; *6*—Cenozoic unconsolidated deposits; and *7*—faults. The rectangle shows the study area. Terranes are labeled with letters: GL —Galam; DZ – Dzhagdy; NL—Nilan; LN —Lan; SK— Selemdzha—Kerbi; TK—Tukuringra; TR—Tokur; UL— Ulban; UB—Un'ya Bom; and YK—Yankan.

The mounts were imaged via BSE using a Hitachi S-3400N scanning electron microscope equipped with a Gatan Chroma CL2 detector. U–Th–Pb geochronological studies on zircons were performed at the University of Arizona LaserChron Center, Department of Geosciences, Tucson, USA. Zircons were ablated using a Photon Machines Analyte G2 excimer laser and a Thermo Scientific Element 2 ICP—MS with a 20-μm-wide laser spot and resulting in a pit 15 μm deep. Calibration was performed relative to the FC zircon standard (Duluth complex, 1099.3 ± 0.3 Ma [51]). Zircons SL (Sri Lanka) and R33 (Braintree complex) were used as secondary standards to control accuracy of measurement [38]. The $^{206}Pb/^{238}U$ and $^{207}Pb/^{206}Pb$ dates for the SL zircon standard are 557 ± 5 and 558 ± 7 Ma (2σ), which is in good agreement with the ID–TIMS ages reported in [42]. The mean $^{206}Pb/^{238}U$ and $^{207}Pb/^{206}Pb$ ages for the R33 standard are 417 ± 7 and 415 ± 8 Ma, which are consistent with the recommended dates in [38, 47]. Systematic errors are 0.9% for $^{206}Pb/^{238}U$ and 0.8% for $^{206}Pb/^{207}Pb$ (2σ). Common-Pb corrections were applied using the Hg-corrected ^{204}Pb and according to the model in [53]. For details of the analytical procedures, see www.laserchron.org. Concordia ages were calculated with Isoplot 3.6 [46].

Lu-Hf isotope analyses of detrital zircons were conducted with a Nu Instruments High-Resolution Multi Collector ICP Mass Spectrometer (Nu HR ICPMS) and a Photon Machines Analyte G2 excimer laser at the University of Arizona Geochronological Center. Instrument settings were established by analyzing standard solutions of JMC475 and Spex Hf and solutions containing Spex Hf, Yb, and Lu. Standard zircons Mud Tank, 91500, Temora, R33, FC52, Plesovice, and Sri Lanka were also analyzed to monitor data quality. Hf isotope analyzes of zircons were made in the same locations as the U–Th–Pb analyses with a laser beam diameter of 40 μm, a laser fluence of ~5 J/cm^2, pulse rate of 7 Hz, and an ablation rate of ~0.8 μm/s. For details of the analytical methodology, see www.laserchron.org. The $\varepsilon_{Hf(t)}$ values were calculated using the decay constant of ^{176}Lu ($\lambda = 1.867e^{-11}$) after [52] and chondritic ratios of $^{176}Hf/^{177}Hf$ (0.282785) and $^{176}Lu/^{177}Hf$ (0.0336) after [39]. Crustal model ages $t_{Hf(C)}$ were calculated assuming an average $^{176}Lu/^{177}Hf = 0.0093$ for the continental crust [37, 56]. Isotope parameters for the depleted mantle were calculated using present-day $^{176}Hf/^{177}Hf = 0.28325$ and $^{176}Lu/^{177}Hf = 0.0384$ [43].

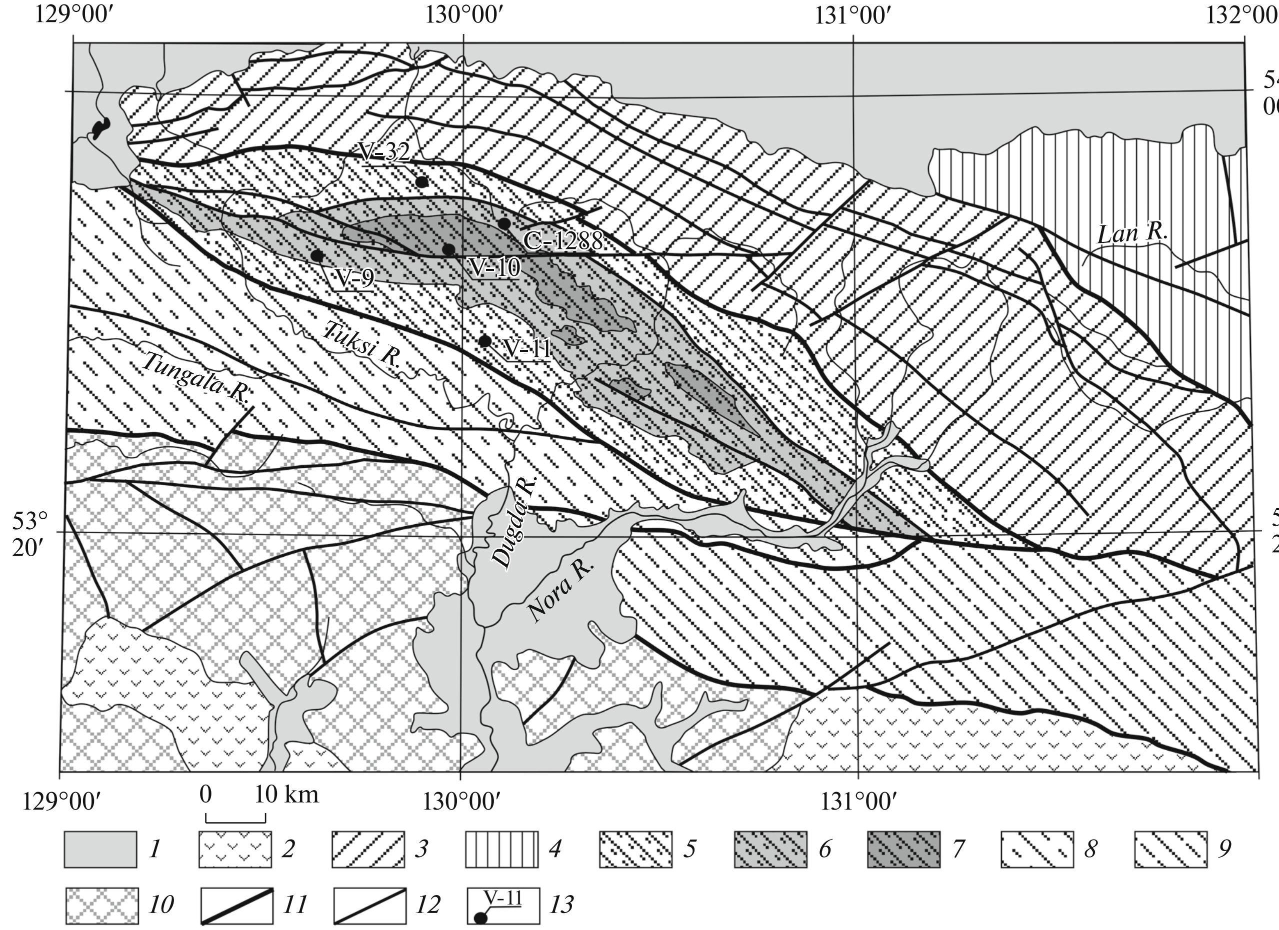

Fig. 2. Schematic geological structure of the eastern part of the Mongol–Okhotsk Fold Belt after [27, 29]. *1*—Cenozoic unconsolidated deposits; *2*—Lower Cretaceous intermediate volcanic rocks; *3*—Upper Triassic and Lower–Middle Jurassic metasedimentary formations of the Un'ya-Bom Terrane; *4*—Carboniferous and Permian metaterrigenous and metavolcanogenic formations of the Lan Terrane; *5*–*7*—Upper Paleozoic metaterrigenous and metavolcanogenic formations of the Dzhagdy Terrane: *5*—presumably Lower Carboniferous Dzheskogon Formation; *6*—Upper Carboniferous Nekter Formation; *7*—Lower Permian Bochagor Formation; *8*—presumably Silurian and Devonian terrigenous and volcanogenic formations of the Dolbyr–Tungala Terrane; *9*—presumably Carboniferous terrigenous and volcanogenic formations of the Selemdzha–Kerbi Terrane; *10*—Paleozoic intrusive and sedimentary assemblages of the northern framing of the Amur Superterrane; *11*—major faults (boundaries between terranes); *12*—minor faults; and *13*—sampling sites for U–Pb geochronological and Lu–Hf isotope studies and their numbers.

OBJECTS OF RESEARCH

As mentioned above, our research is concerned with metasedimentary rocks of Dzhagdy Terrane in the Mongol–Okhotsk Fold Belt. This 35- to 40-km-wide terrane extends in roughly an eastwesterly direction for about 200 km between the Un'ya-Bom and Dolbyr–Tungala terranes (Figs. 1 and 2). The following sequence of stratified rocks is distinguished in its structure (from bottom to top) [27].

The presumably Lower Carboniferous Dzheskogon Formation is 1550 m thick and consists of clay shales alternating with inequigranular polymictic sandstones, greenstone rocks, and limestones lenses. No fauna has been found in the formation. The Early Carboniferous age of the formation is agreed upon considering the fact that the Nekter Formation rests with conformity on its rocks.

The Upper Carboniferous Nekter Formation is 1050-m thick and is formed by phyllitized siltstones, clay shales with interlayers, and lenses of fine-grained polymictic metasandstone, greenschists, quartzite, and marmorized limestones. *Triticites* ex gr. *parvulus* Schell. and *T.* ex gr. *irregularis* Schell. foraminifera characteristic of the end of the Late Carboniferous were found in the limestone of the Nekter Formation. The Nekter Formation is conformably overlain by the Bochagor Formation.

The Lower Permian Bochagor Formation is 1650-m thick and comprises phyllites, greenschists, quartzites, metasandstones with beds, and lenses of chert, mudstones, and marmorized limestones. The foraminiferal and coral assemblages composing *Pseudofusulina* cf. *uralica* Schelw., *Acervoschwagerina* sp., and *Waagenophyllum* cf. *magnificum* Dougl. characteristic of the Asselian stage of the Lower Permian occur in the Bochagor limestones.

Rocks of the above stratigraphic units underwent greenschist–facies metamorphism of varying degrees [15, 27].

The current scientific understanding [15, 27] suggests that the Dzheskogon (at the bottom) and Nekter (at the top) formations shape the flanks of the Tuksi syncline and, the Bochagor Formation, its core. At the same time, according to B.A. Natal'in et al. [23], these formations shape a recumbent anticlinal fold, which implies the inverse age relationships of the rocks. Furthermore, he has identified seven deformation stages in the evolution of Dzhagdy Terrane, resulting in folds and faults of different ages.

U-Pb isotopic studies were conducted on the detrital zircons from all the stratigraphic units of the Dzhagdy Terrane: metasandstones and metasiltstones (Samples V-11 and V-32) of the Dzheskogon Formation, metasandstones and metasiltstones (Samples V-9 and C-1288) of the Nekter Formation, and the sandstone (Sample V-10) of the Bochagor Formation. In addition, we have taken into account the current views on the structure of Dzhagdy Terrane, and samples of the Dzheskogon and Nekter formations were collected from the northern and southern flanks of the fold structure (Fig. 2).

Geochronological studies of the rocks from different formations revealed no differences in their petrographic characteristics. By the size of the fragments, they are represented by layered, rarely massive, metasandstones and metasiltstones. The subangular to subrounded clastic material is represented by quartz and feldspar. A combination of regenerative and blastopsammitic textures is characteristic of clasts.

DETRITAL ZIRCON U-PB GEOCHRONOLOGY

Out of 122 studied detrital zircon grains from the metasandstone of the northern part of the Dzheskogon Formation (Sample V-32) concordant ages were obtained for 91 grains. They are mainly in the interval 218 to 501 Ma. The relative age probability diagram shows peaks in age at 239, 261, 473, and 494 Ma. In addition, there are single zircon grains with concordant ages of ca. 578, 878, 893, 1112, and 1194 Ma.

Concordant ages in the interval 193 to 500 Ma were obtained for 101 grains out of 117 studied detrital zircons from the metasiltstone in the southern part of the Dzheskogon Formation (Sample V-11). The relative age probability diagram shows major age peaks at 196, 256, 449, and 480 Ma (Fig. 3b). There also occur discrete zircon grains with concordant ages ca. 551, 878, 959, and 1431 Ma.

U-Pb geochronological studies on 118 detrital zircon grains from the northern part of the Nekter Formation (Sample C-1288) yielded concordant ages for 96 grains in the interval from 197 to 547 Ma. The relative age probability diagram shows major age peaks at 202, 213, 262, 353, 418, 448, 483, 509, and 543 Ma (Fig. 3c). In addition, there are single zircon grains with concordant ages of ca. 622, 843, and 1806 Ma.

A total of 128 detrital zircon grains were obtained from the southern part of the Nekter Formation (Sample V-9), which yielded concordant ages for 117 grains predominantly in the intervals from 211 to 285 Ma, 456 to 518 Ma, and 739 to 1126 Ma. The relative age probability diagram shows major age peaks at 220, 262, 485, 759, 957, and 1104 Ma. There are also single zircon grains with concordant ages of ca. 559 Ma, 1.4, 1.6, and 1.8 Ga (Fig. 3d).

Geochronological studies on 125 zircon grains from the metasandstone of the Bochagor Formation (Sample V-10) taken from the axial part of Dzhagdy Terrane yielded concordant ages for 116 grains in the interval from 245 Ma to 1.2 Ga. The relative age probability diagram shows major age peaks at 255, 486, 761, 955, and 1122 Ma (Fig. 3e). In addition, there are single zircon grains with concordant ages ca. 1.2, 1.4, and 1.8 Ga.

LU-HF ISOTOPIC RESULTS

Lu-Hf analysis locations were in the same spot as concordant U-Pb spots. In total, 18 to 20 grains from each sample were analyzed. The research results are in Figure 4 and in the table.

From the data it follows that Mesozoic zircons from metaterrigenous rocks of the Dzheskogon, Nekter, and Bochagor formations show generally positive $\varepsilon_{Hf(t)}$ values (up to +11), near zero $\varepsilon_{Hf(t)}$ values, and rarely low negative $\varepsilon_{Hf(t)}$ values (–3) (Fig. 4) These zircons have model ages $t_{Hf(C)}$ of 0.5 to 1.2 Ga.

Paleozoic and Neoproterozoic zircons yield $t_{Hf(C)}$ values as high as 1.6 Ga with $\varepsilon_{Hf(t)}$ values close to those in Mesozoic zircons (Fig. 4).

DISCUSSION

The geochronological data on detrital zircons from metaterrigenous rocks of the Dzhagdy Terrane were quite surprising.

First, the youngest zircon populations in metasedimentary rocks of the Dzheskogon (samples V-11 and V-32) and Nekter (samples V-9 and C-1288) formations are of Early Mesozoic age (Figs. 3a–3d), which conflicts with the opinion in [27] on their Early and Late Carboniferous ages.

Second, the Late Permian age of the youngest zircon population in the metasandstone of the Bochagor Formation (Fig. 3e) indicates an older age for the formation compared to the Nekter and Dzheskogon for-

Table 1. Lu–Hf isotope data on zircons from metasedimentary rocks of Dzhagdy Terrane

Ord. no.	Sample no./Grain no	Age, Ma	$(^{176}Yb + ^{176}Lu)/^{176}Hf$, %	$^{176}Lu/^{177}Hf$	$^{176}Hf/^{177}Hf$	±(1σ)	$\varepsilon_{Hf(t)}$	$t_{Hf(DM)}$	$t_{Hf(C)}$
Metasandstones of the Dzheskogon Formation, northern part of the terrane									
1	V-32/89	235	46.7	0.002807	0.282777	0.000027	4.9	0.7	0.8
2	V-32/57	236	16.3	0.001061	0.282852	0.000017	7.9	0.6	0.7
3	V-32/28	238	16.6	0.001129	0.282839	0.000016	7.4	0.6	0.7
4	V-32/44	240	20.8	0.001402	0.282765	0.000019	4.8	0.7	0.8
5	V-32/25	240	52.4	0.003322	0.282834	0.000023	6.9	0.6	0.7
6	V-32/48	244	31.1	0.001981	0.282787	0.000021	5.6	0.7	0.8
7	V-32/124	245	29.4	0.001917	0.282803	0.000014	6.2	0.7	0.7
8	V-32/117	247	25.6	0.001422	0.282851	0.000017	8.0	0.6	0.7
9	V-32/63	248	14.5	0.000876	0.282727	0.000019	3.7	0.7	0.9
10	V-32/11	250	11.4	0.000755	0.282775	0.000018	5.5	0.7	0.8
11	V-32/41	252	29.1	0.001844	0.282819	0.000021	6.9	0.6	0.7
12	V-32/116	255	49.1	0.002840	0.282777	0.000024	5.3	0.7	0.8
13	V-32/129	256	48.8	0.003003	0.282707	0.000021	2.8	0.8	0.9
14	V-32/22	258	13.4	0.000889	0.282702	0.000019	3.0	0.8	0.9
15	V-32/39	260	13.5	0.000884	0.282670	0.000019	2.0	0.8	1.0
16	V-32/88	262	19.6	0.001215	0.282819	0.000018	7.2	0.6	0.7
17	V-32/40	267	25.2	0.001594	0.282645	0.000019	1.1	0.9	1.0
18	V-32/93	287	33.2	0.001997	0.282631	0.000020	1.0	0.9	1.0
19	V-32/42	471	32.0	0.001957	0.282561	0.000022	2.3	1.0	1.1
20	V-32/73	477	16.1	0.000960	0.282324	0.000022	–5.6	1.3	1.5
Metasiltstones of the Dzheskogon Formation, southern part of the terrane									
21	V-11/80	194	60.4	0.003637	0.282964	0.000020	10.6	0.4	0.5
22	V-11/112	196	62.7	0.003746	0.282903	0.000028	8.4	0.5	0.6
23	V-11/22	197	26.6	0.001668	0.282944	0.000021	10.2	0.4	0.5
24	V-11/93	198	32.4	0.001776	0.282794	0.000016	4.9	0.7	0.8
25	V-11/109	199	33.9	0.002092	0.282876	0.000021	7.8	0.5	0.6
26	V-11/77	201	27.5	0.001640	0.282689	0.000020	1.3	0.8	1.0
27	V-11/2	214	10.1	0.000602	0.282735	0.000016	3.3	0.7	0.9
28	V-11/20	240	37.7	0.002394	0.282852	0.000019	7.7	0.6	0.7
29	V-11/53	251	22.2	0.001370	0.282773	0.000020	5.3	0.7	0.8
30	V-11/30	254	29.5	0.001904	0.282783	0.000023	5.6	0.7	0.8
31	V-11/126	258	20.5	0.001450	0.282824	0.000017	7.3	0.6	0.7
32	V-11/101	265	16.2	0.001166	0.282832	0.000016	7.7	0.6	0.7
33	V-11/107	275	27.6	0.001977	0.282818	0.000021	7.3	0.6	0.7
34	V-11/129	287	21.2	0.001322	0.282754	0.000022	5.4	0.7	0.8
35	V-11/16	339	12.3	0.000900	0.282680	0.000020	4.0	0.8	0.9
36	V-11/90	356	8.7	0.000550	0.282724	0.000020	6.0	0.7	0.8
37	V-11/94	442	10.8	0.000874	0.282422	0.000018	–2.9	1.2	1.4
38	V-11/82	449	40.7	0.002482	0.282430	0.000026	–2.9	1.2	1.4
39	V-11/50	486	8.4	0.000504	0.282409	0.000020	–2.3	1.2	1.4
40	V-11/57	501	11.0	0.000676	0.282567	0.000017	3.6	1.0	1.1

Table 1. (Contd.)

Ord. no.	Sample no./Grain no	Age, Ma	(^{176}Yb + ^{176}Lu)/^{176}Hf, %	$^{176}Lu/^{177}Hf$	$^{176}Hf/^{177}Hf$	±(1σ)	$\varepsilon_{Hf(t)}$	$t_{Hf(DM)}$	$t_{Hf(C)}$
Metasiltstones of the Nekter Formation, northern part of the terrane									
41	C-1288/65	202	20.4	0.001202	0.282585	0.000018	–2.3	0.9	1.2
42	C-1288/21	202	34.1	0.002283	0.282702	0.000029	1.7	0.8	0.9
43	C-1288/42	212	62.9	0.004376	0.282665	0.000050	0.3	0.9	1.0
44	C-1288/105	216	65.1	0.003860	0.282828	0.000024	6.2	0.6	0.7
45	C-1288/87	224	30.9	0.001866	0.282832	0.000025	6.8	0.6	0.7
46	C-1288/83	240	37.9	0.002427	0.282826	0.000021	6.8	0.6	0.7
47	C-1288/91	253	31.2	0.001971	0.282855	0.000020	8.1	0.6	0.7
48	C-1288/11	253	29.4	0.002050	0.282917	0.000023	10.3	0.5	0.5
49	C-1288/82	254	21.9	0.001377	0.282862	0.000023	8.6	0.6	0.6
50	C-1288/18	261	23.0	0.001780	0.282817	0.000029	7.0	0.6	0.7
51	C-1288/122	278	49.9	0.003134	0.282690	0.000026	2.6	0.8	1.0
52	C-1288/73	306	9.8	0.000737	0.282685	0.000020	3.5	0.8	0.9
53	C-1288/54	339	23.7	0.001650	0.282617	0.000024	1.6	0.9	1.1
54	C-1288/103	354	11.0	0.000666	0.282688	0.000019	4.6	0.8	0.9
55	C-1288/98	375	6.7	0.000660	0.282910	0.000024	13.0	0.5	0.5
56	C-1288/113	446	15.0	0.000968	0.282593	0.000021	3.2	0.9	1.1
57	C-1288/93	488	9.9	0.000594	0.282436	0.000021	–1.3	1.1	1.3
58	C-1288/43	506	8.1	0.000564	0.282401	0.000024	–2.2	1.2	1.4
59	C-1288/116	547	13.4	0.000937	0.282267	0.000023	–6.2	1.4	1.6
Metasandstones of the Nekter Formation, southern part of the terrane									
60	V-9/13	212	16.9	0.001084	0.282961	0.000020	11.2	0.4	0.5
61	V-9/34	216	9.2	0.000656	0.282734	0.000017	3.3	0.7	0.9
62	V-9/.128	221	16.5	0.001100	0.282817	0.000020	6.3	0.6	0.7
63	V-9/23	221	17.3	0.001132	0.282676	0.000018	1.3	0.8	1.0
64	V-9/80	232	26.6	0.001747	0.282683	0.000026	1.7	0.8	1.0
65	V-9/54	247	8.4	0.000590	0.282598	0.000018	–0.8	0.9	1.1
66	V-9/123	256	9.5	0.000685	0.282561	0.000017	–2.0	1.0	1.2
67	V-9/9	258	16.7	0.001013	0.282580	0.000021	–1.3	1.0	1.1
68	V-9/27	262	20.3	0.001294	0.282678	0.000017	2.2	0.8	1.0
69	V-9/99	262	20.8	0.001326	0.282536	0.000018	–2.8	1.0	1.2
70	V-9/51	263	18.5	0.001198	0.282698	0.000017	2.9	0.8	0.9
71	V-9/78	266	12.6	0.000787	0.282493	0.000011	–4.2	1.1	1.3
72	V-9/42	268	35.8	0.002218	0.282704	0.000018	3.1	0.8	0.9
73	V-9/120	273	6.4	0.000437	0.282600	0.000018	–0.2	0.9	1.1
74	V-9/33	470	24.5	0.001541	0.282564	0.000021	2.5	1.0	1.1
75	V-9/6	477	22.3	0.001370	0.282597	0.000023	3.9	0.9	1.0
76	V-9/87	494	15.7	0.000929	0.282494	0.000015	0.7	1.1	1.2
77	V-9/130	511	16.9	0.001051	0.282367	0.000014	–3.4	1.3	1.4
78	V-9/82	759	13.5	0.000834	0.282293	0.000020	–0.6	1.3	1.5
79	V-9/122	812	33.9	0.002241	0.282583	0.000022	10.1	1.0	1.0

Table 1. (Contd.)

Ord. no.	Sample no./Grain no	Age, Ma	$(^{176}Yb + ^{176}Lu)/^{176}Hf$, %	$^{176}Lu/^{177}Hf$	$^{176}Hf/^{177}Hf$	$\pm(1\sigma)$	$\varepsilon_{Hf(t)}$	$t_{Hf(DM)}$	$t_{Hf(C)}$
Metasandstones of the Bochagor Formation, axial part of the terrane									
80	V-10/94	245	15.5	0.000948	0.282643	0.000023	0.7	0.9	1.0
81	V-10/105	245	12.9	0.000783	0.282583	0.000025	–1.4	0.9	1.1
82	V-10/12	248	25.9	0.001549	0.282580	0.000023	–1.6	1.0	1.1
83	V-10/106	251	12.5	0.000829	0.282530	0.000017	–3.2	1.0	1.2
84	V-10/4	254	20.4	0.001458	0.282682	0.000030	2.1	0.8	1.0
85	V-10/127	257	26.2	0.001593	0.282559	0.000023	–2.1	1.0	1.2
86	V-10/25	258	13.2	0.000881	0.282631	0.000018	0.5	0.9	1.0
87	V-10/123	260	29.2	0.002019	0.282584	0.000020	–1.3	1.0	1.1
88	V-10/5	262	60.3	0.003608	0.282684	0.000029	2.0	0.9	1.0
89	V-10/27	262	17.9	0.001147	0.282543	0.000023	–2.5	1.0	1.2
90	V-10/114	267	11.9	0.000741	0.282531	0.000016	–2.8	1.0	1.2
91	V-10/23	268	46.4	0.002582	0.282623	0.000021	0.2	0.9	1.1
92	V-10/31	270	13.2	0.000817	0.282558	0.000024	–1.8	1.0	1.2
93	V-10/85	429	12.0	0.000810	0.282758	0.000018	8.7	0.7	0.8
94	V-10/82	496	10.0	0.000566	0.282652	0.000018	6.5	0.8	0.9
95	V-10/3	749	11.3	0.000671	0.282410	0.000018	3.4	1.2	1.3
96	V-10/96	788	15.1	0.000917	0.282208	0.000025	–3.0	1.5	1.6
97	V-10/102	912	14.5	0.000871	0.282379	0.000021	5.7	1.2	1.3

Errors at the 1σ level resulting from $^{176}Hf/^{177}Hf$ measurements correspond to the last significant digits after the decimal point.

mations. These data are not consistent with ideas in [10, 15, 27] that the considered formations form a syncline with the Bochagor Formation in its core. At the same time, we note that, based on the structural data of B.A. Natalyin [23], the Nekter and Dzheskogon formations have previously been assumed to be younger than the Bochagor Formation.

Third, relative probability curves for detrital zircon ages from the rocks of the Dzheskogon (Sample V-32, Fig. 3a) and Nekter (Sample C-1288, Fig. 3c) formations in the northern part of Dzhagdy Terrane differ appreciably from those for these same formations (Sample V-11, Fig. 3b, Sample V-9, Fig. 3d) in the southern part of the terrane (see sampling site locations in Fig. 2). This circumstance calls into question the similarity of these deposits recognized as the Dzheskogon and Nekter formations in the northern and southern parts of Dzhagdy Terrane (or “wings” of a single fold structure).

For these contradictions to be resolved, we must admit that the structure of Dzhagdy Terrane is far more complex than previously thought. Attention is drawn to the combination of shallow terrigenous sediments in the composition of the recognized formations, on the one hand, and argillaceous-siliceous sediments, on the other. The limestones with fauna do not form continuous layers [15, 35], however occur mainly as lenses. In the axial part of the terrane in question, schists and limestones of the Permian Bochagor Formation host a tectonic block of the Early Paleozoic (454 ± 5 Ma) granitoids [31]. Therefore, it cannot be ruled out that the above “lenses” of Paleozoic limestones are olistolithes and olistoplaks in the Late Triassic–Early Jurassic matrix.

Thus, our geochronological data, coupled with the above data, suggest that the Dzheskogon, Nekter, and Bochagor formations of Dzhagdy Terrane do not constitute a single sedimentary sequence [15, 27], but a set of tectonic slices consisting of rocks variable in genesis. Therefore, we are left to agree with the earlier assumption [9, 50] that the terrane in question is a fragment of an accretionary prism. However, we clearly understand the need to undertake structural studies to provide evidence for this thesis.

We next compare our new geochronological data with those already available for the zircons from metasedimentary rocks from the eastern part of the Mongol–Okhotsk Belt. As of now, these data are available for the Yankan and Un’ya–Bom terranes, as well as for the western part of the Tukuringra Terrane (Fig. 1 for location of terranes).

In particular, the relative age probability diagrams for detrital zircons from metasedimentary rocks of the Un’ya–Bom Terrane show the youngest age peaks at

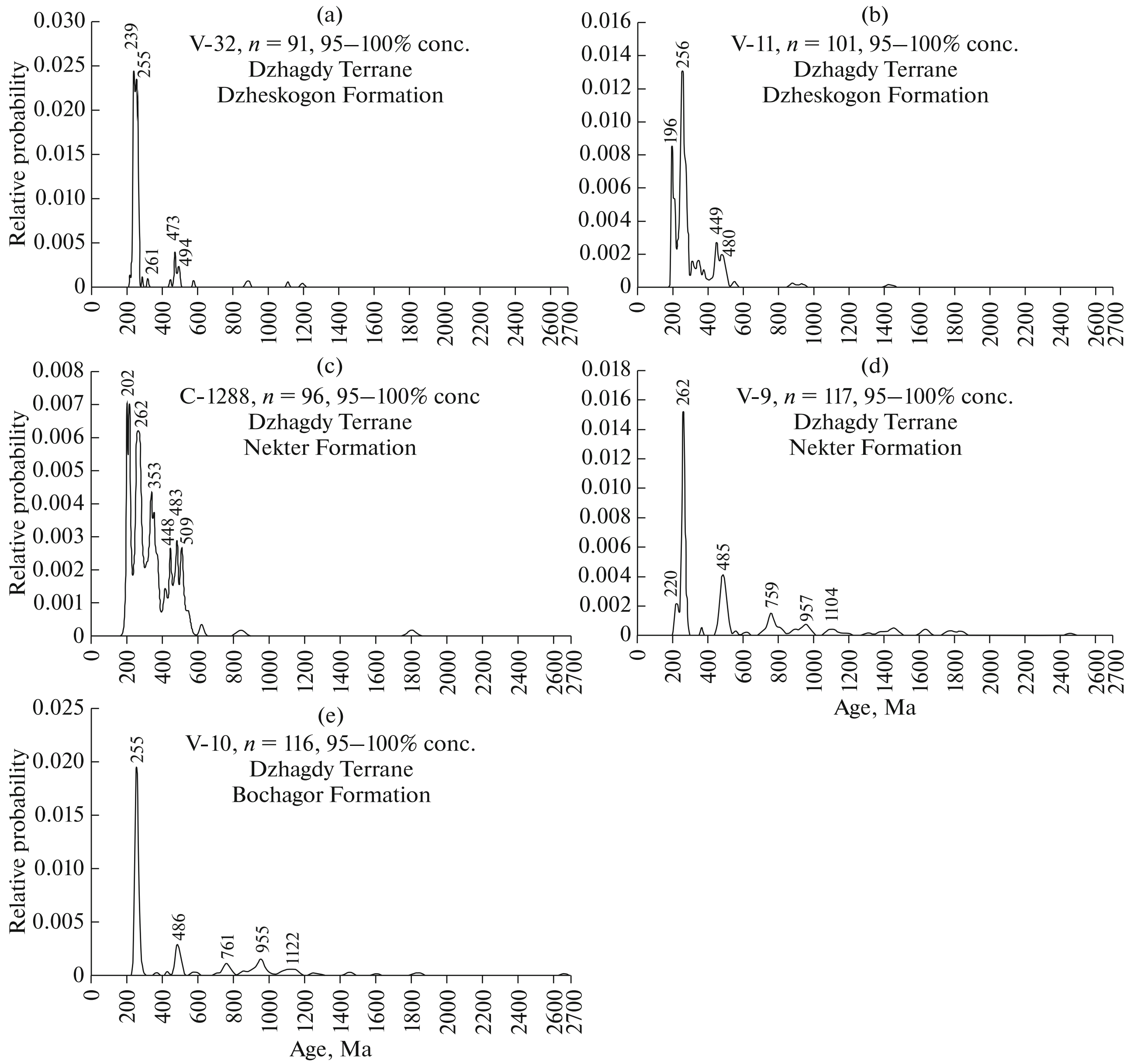

Fig. 3. Relative age probability curves of detrital zircons. (a) metasandstone of the Dzheskogon Formation (Sample V-32); (b) metasiltstone of the Dzheskogon Formation (Sample V-11); (c) metasiltstones of the Nekter Formation (Sample C-1288); (d) metasandstone of the Nekter Formation (Sample V-9); (e) metasandstone of the Bochagor Formation (Sample V-10).

the following: 207 Ma (Kurnal Formation), 212 Ma (Amkan Formation) [14], and 222 Ma (Nel Formation) (unpublished data). Similar estimates were obtained [13] for the youngest age peaks for detrital zircons from metasedimentary rocks in the western part of the Tukuringra Terrane: 185 Ma (Garmakan Formation), 198 Ma (Algaya Formation), and 253 Ma (Teplokluchevskaya Formation) with their Paleozoic age assignment in the published stratigraphic schemes [27]. These data, as well as the findings of this study, indicate that Early Mesozoic sedimentary rocks are more widespread within the eastern part of the Mongol–Okhotsk Belt than is generally agreed. In addition, Early Jurassic zircons in these rocks suggest that sedimentation continued at least until the middle of the Early Jurassic.

At the same time, the youngest zircons from metaterrigenous rocks of the Dzhalinda, Krestovka, and Preobrazhenovkaya formations and the Baldizhak Series of Yankan Terrane are exclusively Paleozoic [33]. This difference in the sources of material for sedimentary rocks of the Yankan Terrane, on the one hand, and the Tukuringra, Un'ya–Bom, and Dzhagha terranes, on the other, is apparently accounted for by the reduction factor of geological complexes in the structure of the Mongol–Okhotsk Belt, which was noted by many researchers [15, 23, 24, 49].

The U-Pb geochronological and Lu-Hf isotopic data on detrital zircons combined with the whole-rock Sm–Nd isotopic composition data from previous studies [12] allow us to characterize the sources of clastic materials for sedimentary rocks assemblages of Dzhagdy Terrane. However, we noted before that the eastern part of the Mongol–Okhotsk Belt borders on the southeastern framing of the North Asian Craton, on the one hand, and the Amur Superterrane (composite massif), on the other (Figs. 1 and 2). Therefore, these structures are potential sources of clastic materials for sedimentary assemblages of the Mongol–Okhotsk Belt, however the structure and isotopic characteristics of the rocks composing them are in sharp contrast. Thus, within the southeastern framing of the North Asian Craton, widely developed are Early Precambrian and younger igneous and metamorphic complexes characterized mainly by Paleoproterozoic and Archean Nd model ages at 3.2–2.0 Ga [4–8, 19] and practically the same Hf model ages at 3.2–1.5 Ga [21].

The geochronological data provide no evidence in support of the involvement of Early Precambrian sedimentary assemblages in the structure of the Amur Superterrane [17, 18, 26, 32, 48, 58, 59], and the oldest Nd-model ages of Neoproterozoic, Paleozoic, and Mesozoic igneous and sedimentary assemblages are, as a rule, Mesoproterozoic (1.5–1.0 Ga) [28, 30, 34].

Turning to the discussion of sources for sediments deposited within Dzhagdy Terrane, we first note that almost all zircons from them yielded no Early Precambrian ages (Fig. 3). Single zircon grains do not form statistically significant populations and are likely recycled material.

As shown earlier [12], metasedimentary rocks of Dzhagdy Terrane have Nd-model age $t_{Nd(DM)}$ of 1.5–1.0 Ga, suggesting that major protoliths of metasedimentary rocks of Dzhagdy Terrane are characterized by Neo- and Mesoproterozoic estimates of the Nd-model ages. In this connection, sedimentary rocks of the terrane in question are assumed [12] to form from the sediment influx mainly from the Amur Superterrane (from the south in present-day coordinates). Contribution from the southern framing of the North Asian Craton (from the north in present-day coordinates) was either insignificant or lacking completely.

As for the Lu-Hf isotopic studies (Fig. 4), an important point is that detrital zircons from metaterrigenous rocks of the Dzheskogon, Nekter, and Bochagor formations show positive, near zero, and low negative $\varepsilon_{Hf(t)}$ values and $t_{Hf(DM)}$ model ages at 1.4 to 0.4 Ga and $t_{Hf(C)}$ model ages at 1.6 to 0.5 Ga. This suggests their origin from reworked crust with Neoproterozoic and Mesoproterozoic Hf isotopic characteristics. We can conclude therefore that detrital zircons in the sedimentation basin were derived from the Amur Superterrane (from the south in present-day coordinates), which is in complete agreement with the conclusion made on the basis of Sm–Nd isotopic characteristics of the metasedimentary rocks.

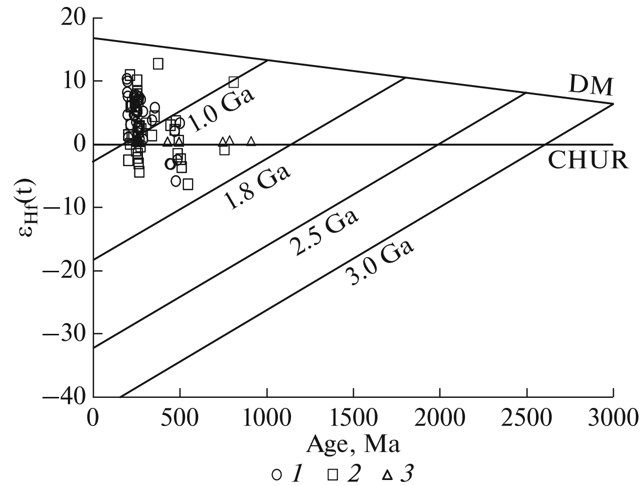

Fig. 4. $\varepsilon_{Hf(t)}$ diagram showing the age (Ma) for zircons from Dzhagdy Terrane metasedimentary rocks. *1–3*—data points of Lu-Hf isotopic compositions of zircons from the following: 1—metasandstones (sample V-32) and metasiltstones (Sample V-11) of the Dzheskogon Formation; *2*—metasiltstones (Sample C-1288) and metasandstones (Sample V-9) of the Nekter Formation; and *3*—metasandstones of the Bochagor Formation (Sample V-10). DM—depleted mantle; CHUR—chondrite uniform reservoir.

CONCLUSIONS

(1) The youngest zircon populations in metasedimentary rocks of the Dzheskogon and Nekter formations have been labeled Middle–Late Triassic and Early Jurassic, suggesting that the formations that were previously assumed to be Carboniferous are Early Mesozoic.

(2) The Early Mesozoic sedimentary assemblages are much more widespread within the eastern part of the Mongol–Okhotsk Belt than generally agreed.

(3) The Dzheskogon, Nekter, and Bochagor formations of Dzhagdy Terrane are not a single sedimentary sequence, but a set of tectonic slices consisting of Late Paleozoic and Early Mesozoic rocks of variable genesis. We cannot rule out that the considered terrane is a fragment of an accretionary prism.

(4) The U-Pb geochronological and Lu-Hf isotopic data on detrital zircons coupled with whole-rock Sm–Nd isotopic composition data from previous studies indicate that sediment influx to the sedimentation basin came mainly from the continental massifs of the Amur Superterrane (from the south in present-day coordinates). Contributions from the southern framing of the North Asian Craton (from the north in pres-

ent-day coordinates) were either insignificant or lacking completely.

ACKNOWLEDGMENTS

The authors are grateful to E.N. Voropaeva, O.G. Medvedeva, and staff at the University of Arizona LaserChron Center, Tucson, USA.

FUNDING

Geological studies were conducted under the Institute of Geology and Nature Management, FEB RAS, research plan (subject matter AA-AA-A16-116051810110-7), and isotope-geochemical and geochronological studies were supported by the Russian Foundation for Basic Research (project 18-05-00206).

REFERENCES

1. I. V. Buchko, A. A. Sorokin, A. E. Izokh, A. M. Larin, A. B. Kotov, E. B. Sal'nikova, S. D. Velikoslavinskii, A. P. Sorokin, S. Z. Yakovleva, and Yu. V. Plotkina, "Petrology of the Early Mesozoic ultramafic-mafic Luchina massif (southeastern periphery of the Siberian craton)," Russ. Geol. Geophys. **49** (8), 570–581 (2008).
2. I. V. Buchko, A. A. Sorokin, E. B. Sal'nikova, A. B. Kotov, S. D. Velikoslavinskii, A. M. Larin, A. E. Izokh, and S. Z. Yakovleva, "The Triassic stage of mafic magmaism in the Dhugdzhur-Stanovoi superterrane (southern framing of the North Asian craton)," Russ. Geol. Geophys. **51** (11), 1157–1166 (2010).
3. I. V. Buchko, A. A. Sorokin, A. B. Kotov, A. V. Samsonov, Yu. O. Larionova, V. A. Ponomarchuk, and A. M. Larin, "The age and tectonic setting of the Lukinda dunite–gabbro–anorthosite massif in the east of the Selenga–Stanovoi superterrane, the Central Asian Fold," Russ. Geol. Geophys. **59** (7), 709–717 (2018).
4. S. D. Velikoslavinskii, A. B. Kotov, E. B. Sal'nikova, A. M. Larin, A. A. Sorokin, A. P. Sorokin, V. P. Kovach, E. V. Tolmacheva, and B. M. Gorokhovskii, "Age of the Ilikan sequence from the Stanovoi Complex of the Dzhugdzhur–Stanovoi Superterrane, Central-Asian Foldbelt," Dokl. Earth Sci. **438** (1), 612–616 (2011).
5. S. D. Velikoslavinskii, A. B. Kotov, E. B. Sal'nikova, A. M. Larin, A. A. Sorokin, A. P. Sorokin, V. P. Kovach, E. V. Tolmacheva, S. Z. Yakovleva, I. V. Anisimova, "Age of the Ust'-Gilyui Sequence in the Stanovoi Complex of the Selenga–Stanovoi Superterrain, Central Asian Fold Belt," Dokl. Earth Sci. **444** (2), 661–665 (2012).
6. S. D. Velikoslavinskii, A. B. Kotov, V. P. Kovach, A. A. Sorokin, A. P. Sorokin, E. V. Tolmacheva, K. L. Wang, and A. B. Sal'nikova, "The Paleoproterozoic age of protoliths of metasedimentary rocks of the Sutam Formation of the Aldan Granulite–Gneiss Megacomplex (Stanovoi Suture)," Dokl. Earth Sci. **463** (2), 765–769 (2015).
7. S. D. Velikoslavinskii, A. B. Kotov, V. P. Kovach, E. V. Tolmacheva, A. M. Larin, A. A. Sorokin, A. P. Sorokin, K. L. Van, and E. B. Salnikova, "Age, sources, and provenances of protoliths of metasedimentary rocks of the Dzheltulak Group, Dzheltulak Suture," Dokl. Earth Sci. **468** (2), 545–548 (2016).
8. S. D. Velikoslavinskii, A. B. Kotov, V. P. Kovach, A. M. Larin, A. A. Sorokin, A. P. Sorokin, E. V. Tolmacheva, E. B. Sal'nikova, K. L. Van, B. M. Jahn, and S. L. Cung, "Mesozoic age of the Gilyui metamorphic complex in the junction zone of the Selenga–Stanovoi and Dzhugdzhur–Stanovoi Superterranes, Central Asian Fold Belt," Dokl. Earth Sci. **468** (2), 561–565 (2016).
9. *Geodynamics, Magmatism, and Metallogeny of East Russia,* Ed. by A.I. Khanchuk (Dal'nauka, Vladivostok, 2006) [in Russian].
10. *Geological Map of the Amr Region and Adjacent 1 : 2500000,* Ed. by L. I. Krasnyi (VSEGEI, St. Petersburg, 1999) [in Russian].
11. A. N. Didenko, V. B. Kaplun, Yu. F. Malyshev, and B. F. Shevchenko, "Lithospheric structure and Mesozoic geodynamics of the eastern Central Asian Fold Belt," Russ. Geol. Geophys. **51** (5), 492–506 (2010).
12. V. A. Zaika, A. A. Sorokin, and V. P. Kovach, "Sources and povenances of the Upper Paleozoic metasedimentary rocks of the Dzhagdy terrane of the Mongol–Okhotsk Fold Belts: results of Sm-Nd isotope-geochemical studies," Geodynamics & Tectonophysics **9** (4), 1331–1338 (2018).
13. V. A. Zaika, A. A. Sorokin, B. Syu, A. B. Kotov, V. P. Kovach, "Geochemical features and sources of metasedimentary rocks of the western part of the Tukuringra terrane of the Mongol–Okhotsk Fold Belt," Stratigraphy. Geol. Correlation **26** (2), 157–178 (2018).
14. V. A. Zaika, A. A. Sorokin, V. P. Kovach, A. P. Sorokin, and A. B. Kotov, Age and sources of the Lower Mesozoic metasedimentary rocks of the Un'ya–Bom terrane in the Mongol–Okhotsk fold belt: results of the U-Th-Pb geochronological (LA–ICP–MS) and Sm-Nd isotope studies," Dokl. Earth Sci. **484** (4), 455–459 (2019).
15. G. L. Kirillova and M. T. Turbin, *Formations and Tectonics of the Dzhagdy Chain of the Mongol–Okhotsk Fold Area* (Nauka, Moscow, 1979) [in Russian].
16. V. D. Kozlov, S. V. Efremov, S. I. Dril', and G. P. Sandimirova, "Geochemistry, isotopic geochronology, and genesis of the Verkhnyaya Unda granitoid batholith," Geochem. Int. **41** (4), 364–378 (2003).
17. A. B. Kotov, A. A. Sorokin, E. B. Sal'nikova, A. P. Sorokin, A. M. Larin, S. D. Velikoslavinskii, T. V. Belyakov, I. V. Anisimova, and S. Z. Yakovleva, "Mesozoic age of granitoids from the Beket Complex (Gonzha Block within the Argun Terrane of the Central-Asian Fold Belt)," Dokl. Earth Sci. **429A** (9), 1457–1461 (2009).
18. A. B. Kotov, A. M. Mazukabzov, T. M. Skovitina, S. D. Velikoslavinsky, A. A. Sorokin, and A. P. Sorokin, " Structural Evolution and Geodynamic Position of the Gonzha Block, Upper Amur Region," Geotectonics **47** (5), 351–361 (2013).
19. A. B. Kotov, S. D. Velikoslavinskii, V. P. Kovach, A. A. Sorokin, A. P. Sorokin, T. M. Skovitina,

N. Yu. Zagornaya, K. L. Wang, S. L. Chung, and B. M. Jahn, "Paleoproterozoic age of the Zeya Group, Stanovoy Complex of the Dzhugdzhur–Stanovoy Superterrane (Central Asian Mobile Belt): results of Sm-Nd isotopic and U-Th-Pb geochronological (LA-ICP-MS) analyses," Dokl. Earth Sci. **471** (2), 1234–1237 (2016).

20. A. M. Larin, A. B. Kotov, E. B. Sal'nikova, A. A. Sorokin, A. P. Sorokin, A. M. Korshunov, S. D. Velikoslavinskii, S. Z. Yakovleva, and Yu. V. Plotkina, "Age and tectonic position of granites and volcanics in the eastern margin of the Selenga–Vitim Volcano-Plutonic Belt," Dokl. Earth Sci. **441** (1), 1502–1507 (2011).
21. A. M. Larin, A. B. Kotov, E. B. Sal'nikova, V. P. Kovach, G. V. Ovchinnikova, V. M. Savatenkov, S. D. Velikoslavinskii, A. A. Sorokin, I. M. Vasil'eva, N. A. Sergeeva, N. N. Mel'nikov, K.-L. Wang, and S.-L. Chun, "Granitoids of the Pozdnestanovoy Complex of the Dzhugdzhur–Stanovoy Superterrane, Central Asia Fold Belt: age, tectonic setting, and sources," Petrology **26** (5), 447–468 (2018).
22. D. V. Metelkin, I. V. Gordienko, and V. S. Klimuk, "Paleomagnetism of Upper Jurassic basalts from Transbaikalia: new data on the time of closure of the Mongol–Okhitsk Ocean and Mesozoic intraplate tectonics of Central Asia," Russ. Geol. Geophys. **48** (10), 825–834 (2007).
23. B. A. Natal'in, L. I. Popeko, and S. A. Chebotov, "Tectonics of the West Dzhagdy Zone of the Mongol–Okhotsk Fold System," Tikhookean. Geol. **4** (2), 49–64 (1985).
24. L. M. Parfenov, L. I. Popeko, and O. Tomurtogoo, "Problems of tectonics of the Mongol–Okhotsk Orogenic Belt," Tikhookean. Geol. **18** (5), 24–43 (1999).
25. E. B. Sal'nikova, A. M. Larin, A. B. Kotov, A. P. Sorokin, A. A. Sorokin, S. D. Velikoslavinskii, S. Z. Yakovleva, A. M. Fedoseenko, and Yu. V. Plotkina, "The Toksko–Algomin igneous complex of the Dzhugdzhur–Stanovoi folded region: age and geodynamic setting," Dokl. Earth Sci. **409** (5), 888–892 (2006).
26. E. B. Sal'nikova, A. B. Kotov, V. P. Kovach, S. D. Velikoslavinskii, B. M. Jah, A. A. Sorokin, A. P. Sorokin, K. L. Wang, S. L. Chung, H. Y. Lee, and E. V. Tolmacheva, "Age of the Gonzha Group (Argun Terrane, Central Asian Fold Belt) Inferred from U–Pb and Lu–Hf Zircon Data," Dokl. Earth Sci. **444** (5), 692–695 (2012).
27. A. N. Serezhnikov and Yu. R. Volkova, *State Geological Map of the Russian Federation . 1 : 1000000. 3rd Generation. Sheet N-52 (Zeya). Dal'nevostochnaya Series,* Ed. by A.S. Vol'skii (VSEGEI, St. Petersburg, 2007) [in Russian].
28. Yu. N. Smirnova, A. A. Sorokin, L. I. Popeko, A. B. Kotov, V. P. Kovach, "Geochemistry and provenances of the Jurassic terrigenous rocks of the Upper Amur and Zeya–Dep troughs, eastern Central Asian Fold Belt," Geochem. Int. **55** (2), 163–183 (2017).
29. A. A. Sorokin, N. M. Kudryashov, A. P. Sorokin, A. G. Rublev, O. A. Levchenkov, A. B. Kotov, E. B. Sal'nikova, and V. P. Kovach, "Geochronology, geochemistry, and geodynamic setting of Paleozoic granitoids in the eastern segment of Mongol–Okhotsk Belt," Dokl. Earth Sci. **393** (8), 1136–1140 (2003).
30. A. A. Sorokin, A. B. Kotov, N. M. Kudryashov, and V. P. Kovach, "Late Paleozoic Urusha magmatic complex in the southern framing of the Mongolia–Okhotsk Belt (Amur Region): age and geodynamic setting," Petrology **13** (6), 596–610 (2005).
31. A. A. Sorokin, A. B. Kotov, E. B. Sal'nikova, N. M. Kudryashov, and V. P. Kovach, "Early Paleozoic gabbro-granitoid associations in eastern segment of the Mongolian–Okhotsk Fold belt (Amur River Basin): age and tectonic position," Stratigraphy. Geol. Correlation. **15** (3), 241–257 (2007).
32. A. A. Sorokin, Yu. V. Smirnov, A. B. Kotov, E. B. Sal'nikova, A. P. Sorokin, V. P. Kovach, S. Z. Yakovleva, and I. V. Anisimova, "Early Paleozoic age of the Isagachi Sequence (Chalaya Group, Gonzha Terrane) in the eastern part of the Central Asian Fold Belt," Dokl. Earth Sci. **457** (1), 810–813 (2014).
33. A. A. Sorokin, A. A. Kolesnikov, A. B. Kotov, A. P. Sorokin, V. P. Kovach, "Sources of detrital zircons from terrigenous deposits in the Yankan Terrane of the Mongolian–Okhotsk Mobile Belt," Dokl. Earth Sci. **462** (2), 621–625 (2015).
34. A. A. Sorokin, Yu. N. Smirnova, A. B. Kotov, V. P. Kovach, E. B. Sal'nikova, and L. I. Popeko, "Provenances of the Paleozoic terrigenous sequences of the Oldoi Terrane of the Central Asian Orogenic Belt: Sm–Nd isotope geochemistry and U–Pb geochronology (LA–ICP–MS)," Geochem. Int. **53** (6), 534–544 (2015).
35. M. T. Turbin, *Geological Map of the USSR. 1:200 000. Amur–Zeya Series. N-52-XXII*, Ed. by L.B. Krivitskii (VSEGEI, Moscow, 1977) [in Russian].
36. A. A. Tsygankov, B. A. Litvinovsky, B. M. Jahn, M. Reichow, D. I. Liu, A. N. Larionov, S. L. Presnyakov, E. N. Lepekhina, and S. A. Sergeev, "Sequence of magmatic events in the Late Paleozoic of Transbaikalia, Russia (U-Pb isotope data)," Russ. Geol. Geophys. **51** (9), 972–994 (2010).
37. Y. Amelin and W. J. Davis, "Geochemical test for branching decay of ^{176}Lu," Geochim. Cosmochim. Acta **69**, 465–473 (2005).
38. L. P. Black, S. L. Kamo, C. M. Allen, D. W. Davis, J. N. Aleinikoff, J. W. Valley, R. Mundil, I. H. Campbell, R. J. Korsch, I. S. Williams, and C. Foudoulis, "Improved ^{206}Pb/^{238}U microprobe geochronology by the monitoring of trace-element-related matrix effect: SHRIMP, ID-TIMS, ELA-ICP-MS and oxygen isotope documentation for a series of zircon standards," Chem. Geol. **205**, 115–140 (2004).
39. A. Bouvier, J. D. Vervoort, and J. Patchett, "The Lu-Hf and Sm-Nd isotopic composition of CHUR: constraints from unequilibrated chondrites and implications for the bulk composition of terrestrial planets," Earth Planet. Sci. Lett. **273**, 48–57 (2008).
40. D. Bussien, N. Gombojav, W. Winkler, and A. Quadt, "The Mongol-Okhotsk Belt in Mongolia - an appraisal of the geodynamic development by the study of sandstone provenance and detrital zircons," Tectonophysics **510**, 132–150 (2011).
41. T. V. Donskaya, D. P. Gladkochub, A. M. Mazukabzov, and A. V. Ivanov, "Late Paleozoic–Mesozoic subduction-related magmatism at the southern margin of the Siberian Continent and the 150-million-year histo-

ry of the Mongolia–Okhotsk Ocean," Asian J. Earth Sci. **62**, 79–97 (2013).

42. G. E. Gehrels, V. Valencia, and J. Ruiz, "Enhanced precision, accuracy, efficiency, and spatial resolution of U-Pb ages by laser ablation-multicollector-inductively coupled plasma-mass spectrometry," Geochem., Geophys., Geosyst. **9** (3), 1–13 (2008).
43. W. L. Griffin, E. A. Belousova, S. R. Shee, and N. J. Pearson, and S. Y. O'Reilly, "Archean crustal evolution in the northern Yilgarn Craton: U-Pb and Hf-Isotope evidence from detrital zircons," Precambrian Res. **131**, 231–282 (2004).
44. T. K. Kelty, A. Yin, B. Dash, E. George, F. Gehrels, and Angela E. Ribeiro, "Detrital-zircon geochronology of Paleozoic sedimentary rocks in the Hangay–Hentey Basin, North-Central Mongolia: implications for the tectonic evolution of the Mongol-Okhotsk Ocean in Central Asia," Tectonophysics **451**, 290–311 (2008).
45. A. I. Khanchuk, A. N. Didenko, L. I. Popeko, A. A. Sorokin, and B. F. Shevchenko, "Structure and evolution of the Mongol-Okhotsk Orogenic Belt," *The Central Asian Orogenic Belt. Geology, Evolution, Tectonics, and Models*, Ed. by Kr@oner Alfred, (Borntraeger Sci. Publ, Stuttgart, 2015), pp. 211–234.
46. K. R. Ludwig, Isoplot 3.6: Berkeley Geochronol. Center Spec. Publ., no. 4, (2008).
47. J. M. Mattinson, "Analysis of the Relative Decay Constants of ^{235}U and ^{238}U by Multi-Step CA-TIMS Measurements of Closedsystem Natural Zircon Samples," Chem. Geol. **275**, 186–198 (2010).
48. L. Miao, F. Zhang, M. Zhu, and D. Liu, "Zircon SHRIMP U-Pb dating of metamorphic complexes in the conjunction of the Greater and Lesser Xing'an Ranges, NE China: timing of formation and metamorphism and tectonic implications," J. Asian Earth Sci. **114**, 634–648 (2015).
49. "History and modes of mesozoic accretion in southeastern Russia," The Island Arc **2**, 15–34 (1993).
50. W. J. Nokleberg, T. K. Bundtzen, R. A. Eremin, V. V. Ratkin, K. M. Dawson, V. I. Shpikerman, N. A. Goryachev, S. G. Byalobzhesky, Y. F. Frolov, A. I. Khanchuk, R. D. Koch, J. W. H. Monger, A. I. Pozdeev, I. S. Rozenblum, S. M. Rodionov, L. M. Parfenov, C. R. Scotese, and A. A. Sidorov, *Metallogenesis and Tectonics of the Russian Far East, Alaska, and the Canadian Cordillera*, Prof. Pap.-US Geol. Surv., No. 1697, (2005).
51. J. B. Paces and J. D. Miller, "Precise U-Pb ages of Duluth Complex and related mafic intrusions, northeastern Minnesota: geochronological insights to physical, petrogenic, paleomagnetic, and tectonomagmatic processes associated with the 1.1. Ga Midcontinent Rift System," J. Geophys **98** (8), 13997–14013 (1993).
52. U. Soderlund, P. J. Patchett, J. D. Vervoort, and C. E. Isachsen, "The ^{176}Lu decay constant determined by Lu-Hf and U-Pb isotope systematics of Precambrian mafic intrusions," Earth Planet. Sci. Lett. **219**, 311–324 (2004).
53. J. S. Stacey and I. D. Kramers, "Approximation of terrestrial lead isotope evolution by a two-stage model," Earth Planet. Sci. Lett. **26** (2), 207–221 (1975).
54. D. Y. Sun, J. Gou, T. H. Wang, Y. S. Ren, Y. J. Liu, H. Y. Guo, X. M. Liu, and Z. C. Hu, "Geochronological and geochemical constraints on the Erguna Massif basement, NE China - subduction history of the Mongol–Okhotsk oceanic crust," Int. Geol. Rev. **55** (14), 1801–1816 (2013).
55. J. Tang, W. L. Xu, F. Wang, S. Zhao, W. Wang, "Mesozoic southward subduction history of the Mongol–Okhotsk oceanic plate: evidence from geochronology and geochemistry of Early Mesozoic intrusive rocks in the Erguna Massif, NE China," Gondwana Res. **31**, 218–240 (2016).
56. J. D. Vervoort and P. J. Patchett, "Behavior of hafnium and neodymium isotopes in the crust: constraints from Precambrian crustally derived granites," Geochim. Cosmochim. Acta **60**, 3717–3723 (1996).
57. T. Wang, Y. Tong, L. Zhang, S. Li, H. Huang, Zhang J. Jianjun, L. Guo, Q. Yang, D. Hong, T. Donskaya, D. Gladkochub, and N. Tserendash, "Phanerozoic granitoids in the central and eastern parts of Central Asia and their tectonic significance," J. Asian Earth Sci. **145**, 368–392 (2017).
58. M. J. Xu, W. L. Xu, F. Wang, and F. H. Gao, "Age, association and provenance of the "Neoproterozoic" Fengshuigouhe Group in the Northwestern Lesser Xing'an Range, NE China: constraints from zircon U-Pb geochronology," J. Earth Sci. **23** (6), 786–801 (2012).
59. J. B. Zhou, S. A. Wilde, X. Z. Zhang, S. M. Ren, C. Q. Zheng, "Early Paleozoic metamorphic rocks of the Erguna Block in the Great Xing'an Range, NE China: evidence for the timing of magmatic and metamorphic events and their tectonic implications," Tectonophysics **499**, 105–117 (2011).

Recommended for publishing by G.L. Kirillova
Translated by T. Koryakina